ИНСТИТУТ ЯДЕРНОЙ ФИЗИКИ СО АН СССР

INSTITUTE OF NUCLEAR PHYSICS

V.M.Khatsymovsky

ANALYSIS OF HYPERON NON-LEPTONIC AMPLITUDES WITH THE HELP OF QCD SUM RULES
I. THREE-POINT CORRELATOR

PREPRINT 84-107

НОВОСИБИРСК

ANALYSIS OF HYPERON NON-LEPTONIC AMPLITUDES WITH THE HELP OF QCD SUM RULES

I. THREE-POINT CORRELATOR

V.M.Khatsymovsky

Institute of Nuclear Physics,
630090, Novosibirsk, U.S.S.R.

ABSTRACT

The correlator of two quark currents with baryon quantum numbers and of one four-fermion current is analysed in detail in quantum chromodynamics. The non-zero mean vacuum values of the field operator products are taking into account. Leading order in α_s is considered. The sum rules are obtained which being saturated by the lower baryon states enable one to find the matrix elements of H_w between octet baryons. According to PCAC, this is equivalent to finding S-wave hyperon nonleptonic amplitudes in the soft pion approximation. Results confirm some model calculations and after taking into account another contributions allow one to fit to experimental S-waves. Matrix elements of H_w obtained give also quite reasonable values for the P-waves in the ground-state pole approximation.

1. Introduction

Nowadays, the QCD sum rules (SR) method suggested in ref. [1] is widely used for describing hadron properties. The masses of mesons [1], of baryons [2,3], formfactors and meson coupling constants 4 have been calculated with this method. In ref. [5] the QCD SR for polarization operator of nucleon current in external electromagnetic field have been formulated which enabled one to calculate proton and neutron magnetic moments. In ref. [6], using analogous SR in external axial field, the axial constants of octet baryons were calculated.

In this paper the QCD SR method is used to determine the matrix elements of weak hamiltonian H_w between octet baryons, $\langle B_2 | H_w | B_1 \rangle$. Their knowledge is equivalent to knowledge of S-waves in the soft pion limit once PCAC is used.

The method is based on consideration of three-point vertex function of two baryon currents $\bar{\eta}_1, \eta_2$ and one four-fermion one, H_w. The momenta of $\bar{\eta}_1, \eta_2$ lay in the deep Euclidean region. To write down the double dispersion relation the light-like momentum $l \neq 0$ is introduced into the weak vertex. The calculation of the vertex function in the leading order in α_s with the help of operator product expansion (OPE) can be performed in the usual way (if one restricts himself to $d \leq 6$ operators) by computing Feynman graphs with some of the quark and gluon fields substituted by soft vacuum ones. Other fields are hard and can be considered as perturbative ones due to asymptotic freedom. Infra-red (IR) stability (at $l^2 = 0$) of corresponding Feynman integrals is ensured by four-fermionic character of weak vertex. At $d \geq 7$ these integrals are IR divergent. But at $d = 7,8$ they diverge only logarithmically and can be estimated by introducing reasonable IR cut-off, without detailed knowledge of the long distance dynamics.

The paper is organized as follows. In the next section the method is described. In sect. 3 currents are specified and possible values of α_s-corrections are suggested. In sect. 4 considered are 1) the choice of γ-matrix structures in correlator at formulating SR and 2) consequence of the latter for

the matrix elements of parity violating part of H_W. In sect. 5 the most reliable SR are examined. In sect. 6 violations of both the $SU(3)$ symmetry and Pati-Woo theorem are taken into account. S-waves in the soft pion limit and P-waves in the ground-state pole approximation are found. In sect. 7 selfconsistency of the SR is shown. In sect. 8 we conclude.

2. The method

The correlator of interest has the form

$$K = \int \langle 0|T\{\eta_2(y) H_W(0) \bar{\eta}_1(x)\}|0\rangle \exp(iq_2 y - iq_1 x)\, d^4x\, d^4y \qquad (1)$$

where $\bar{\eta}_1$, η_2 are baryon currents. To determine matrix element $\langle B_2|H_W|B_1\rangle$ we must single out physical states in (1) in two channels. So we need the double dispersion relation for K. To obtain it one should consider the variables q_1^2, q_2^2 as independent, i.e. put $l = q_1 - q_2 \neq 0$. The value extracted from SR is then the function of l^2, and we are interested in the case $l^2 = 0$. OPE is effective, generally speaking, at $S_1 = -q_1^2 \gg 0$, $S_2 = -q_2^2 \gg 0$, $Q^2 = -l^2 \gg 0$. However, as was mentioned in the introduction, power corrections due to $d \leq 8$ operators can be found in the usual way even at $l^2 = 0$.

SR are obtained if the correlator found by insertion of the physical states B_{1i}, B_{2j} is equated with that given by OPE (and represented here in the dispersion form):

$$\sum_{i,j} \tilde{\beta}_{2j}\tilde{\beta}_{1i}(-\gamma_5)\frac{i}{\not p_2 - m_2}\alpha_{ji}\frac{i}{\not p_1 - m_1}\gamma_5 = \sum_{i=0}^{3} T_i \int_0^\infty\int_0^\infty \frac{\rho_i(S_1', S_2')\, dS_1' dS_2'}{(S_1'+S_1)(S_2'+S_2)} \qquad (2)$$

Here $\tilde{\beta}_{1i}$, $\tilde{\beta}_{2j}$ are residues of B_{1i}, B_{2j} into currents η_1, η_2: $(2\pi)^2\langle 0|\eta|B\rangle = \tilde{\beta}\gamma_5 u$, where baryon spinor u is normalized as $\bar{u}u = 2m$. $\langle B_{2j}|H_W|B_{1i}\rangle = \alpha_{ji}\bar{u}_j u_i$, $\rho_i(S_1, S_2)$ are

some scalar spectral functions, and all the spin structure is absorbed in matrices T_i:

$$T_0 = \not p_1 - \not p_2,\quad T_1 = \not p_1 + \not p_2,\quad T_2 = \tfrac{1}{2}[\not p_2, \not p_1],\quad T_3 = 1 \qquad (3)$$

For simplicity, we have included in (2) only one-particle intermediate states $J^P = \frac{1}{2}^+$ and parity conserving part H_W^{PC} of H_W (H_W^{PV} is considered further, see sect. 4).

Apply the double Borel transformation [4] to the coefficients of T_i in (2). The former is defined for the scalar function $f(S_1, S_2)$ as

$$f(t_1,t_2) = \frac{1}{(2\pi i)^2}\int_{c-i\infty}^{c+i\infty}\exp\left(\frac{S_1}{t_1}\right)\frac{dS_1}{t_1}\int_{c-i\infty}^{c+i\infty}\exp\left(\frac{S_2}{t_2}\right)\frac{dS_2}{t_2} f(S_1, S_2) \qquad (4)$$

where $c > 0$. The Borel transformation improves convergence of OPE series. It also suppresses the contribution of higher resonances in (2), therefore at the first step we can confine ourself to the lower states in (2):

$$\frac{\tilde{\beta}_1\tilde{\beta}_2}{t_1 t_2}\exp\left(-\frac{m_1^2}{t_1} - \frac{m_2^2}{t_2}\right)\alpha_{21}\left[T_2 - \frac{m_1+m_2}{2}T_1 - \frac{m_1-m_2}{2}T_0 + \frac{1}{2}(m_1+m_2)^2 T_3\right] = \sum_{i=0}^{3} T_i \int_0^\infty \frac{dS_2}{t_2}\int_0^\infty \frac{dS_1}{t_1}\rho_i(S_1,S_2)\cdot \exp\left(-\frac{S_1}{t_1} - \frac{S_2}{t_2}\right) \qquad (5)$$

At the second step the higher states are taken into account in a model way as continuum. To do this we restrict the integration in (5) to some region Ω in the quadrant $S_1 \geq 0$, $S_2 \geq 0$. Two variants for Ω are considered:

$$S_1 + S_2 < 2S_0 \quad \text{(triangle)} \qquad (6a)$$

and

$$S_1 < S_{10},\ S_2 < S_{20} \quad \text{(square)} \qquad (6b)$$

α_{21} is defined by (5) as a function of t_1, t_2. Further, the thresholds S_0 or S_{10}, S_{20} are chosen at which the region of practical constancy of $\alpha_{21}(t_1, t_2)$ exists. t_1, t_2 must be sufficiently large in this region to ensure the small-

ness of power corrections. The difference between the values of α_{21} obtained with two choices of Ω (6a,b) doesn't exceed 10% for each structure T_i considered.

3. Currents

Consider in more detail the currents η_1, η_2, H_W entering (1).

Baryon currents η_1, η_2 are three-quark operators without derivatives. Proton current is of the form

$$\eta_p = (u^a C\gamma_\mu u^b)\gamma^\mu d^c \varepsilon_{abc}, \quad C = \gamma_0\gamma_2 \qquad (7)$$

Other currents are obtained from it by SU(3) transform. The SR for corresponding residues of baryons with the exception of Λ case were obtained earlier [2]. They are given in Appendix A.

The structure of the effective hamiltonian for non-leptonic decays $H_W(Q_q)$ is defined by the typical quark momentum Q_q. Q_q is substituted by M at the Borel transformations, Here M^2 is some scale of order of t_1, t_2. Since $M \sim 1\,GeV \sim m_c$, the result of ref. [8] is valid (with notations of ref. [10]):

$$H_W(M) = \sqrt{2}Gcs\,[a_3(M)I_3 + a_6(M)I_6]$$
$$I_3 = (\bar d\gamma_\mu u_L)(\bar u\gamma^\mu s_L) - (\bar u\gamma_\mu u_L)(\bar d\gamma^\mu s_L)$$
$$I_6 = (\bar d\gamma_\mu u_L)(\bar u\gamma^\mu s_L) + (\bar u\gamma_\mu u_L)(\bar d\gamma^\mu s_L) \qquad (8)$$
$$a_i(M) = (\alpha_s(M)/\alpha_s(m_W))^{\lambda_i},\ \lambda_3 = \frac{4}{9} = -2\lambda_6$$
$$c = \cos\theta_c,\ s = \sin\theta_c$$

Further, make some explanations concerning accounting for the so-called "penguin" mechanism considered in [9]. Graphs occuring at calculation of the correlator (1) can be divided into two types, A and B (see figs. 1a and b, respectively). Each cut between H_W and η_1, η_2 intersects four fermion lines in graphs A (in the regime when all the quarks are hard), and

can intersect only two such lines in graphs B. It is easy to see that graphs B are due to the "penguin". Contribution of distances x at which H_W goes away is proportional to x^{-12} in case A (each fermion line gives factor of x^{-3}); it can be proportional to x^{-6} in case B (when the above mentioned cut doesn't intersect gluon lines at all, as in fig. 1b). Thus, the case B as compared to A is characterized by enhanced contribution of large distances. Therefore the statement made in introduction and concerning I R stability of OPE coefficients at $d \leqslant 6$ is valid for class A of diagrams.

Possible is the separate studying of A and B S-wave pieces, since there exists the weak transition $\Xi^- \to \Sigma^-$ contributed only by graphs B (see fig. 1b). Graphs of the leading order in α_s studied in this paper determine the dominant contribution into A piece. Graphs B occur in the next order in α_s but the corresponding loop smallness can be compensated by the contribution of large distances x. We use the experimental fit from $\Xi^- \to \Sigma^-\pi^0$ decay obtained in the way analogous to that used in ref. [9] in analysis of operators $\mathcal{O}_{5,6}$ ($\mathcal{O}_{5,6}$ originate the graphs like that of fig. 2). The relations between the contributions of graphs of fig. 1b into different transitions in the baryon octet are the same as these for the separable contributions of $\mathcal{O}_{5,6}$ in SU(3) limit. It is explained by the similar structure of graphs of fig. 1b and fig. 2. Namely, write down for the s-wave piece B:

$$\sqrt{3}\,\frac{A(\Sigma^+_o)_B}{m_\Sigma - m_N} = -\frac{A(\Lambda^o_-)_B}{m_\Lambda - m_N} = +\frac{A(\Xi^-_-)_B}{m_\Xi - m_\Lambda} \qquad (9)$$

where masses are introduced in order to keep these relations true for separable contributions (of $\mathcal{O}_{56}$) at the low normalization point of H_W. Then write down, following [9], the SU(3) - expression for $A(\Xi^- \to \Sigma^-\pi^0)$:

$$A(\Xi^- \to \Sigma^-\pi^0) = \sqrt{3}\,[A(\Xi^-_-) + A(\Lambda^o_-)] - A(\Sigma^+_o) = \qquad (10)$$
$$= -0.58 = \sqrt{3}\,[A(\Xi^-_-)_B + A(\Lambda^o_-)_B] - A(\Sigma^+_o)_B$$

then

$$A(\Sigma^+_o)_B = +0.91,\ A(\Lambda^o_-)_B = -1.10,\ A(\Xi^-_-)_B = +1.29 \qquad (11)$$

Hereafter A and B pieces will be referred to as I_3 and "penguin" ones, respectively.

4. γ-matrix structures in the correlator.

4.1. Parity conserving part of the correlator

The structure $T_0 = \hat{q}_1 - \hat{q}_2$ enters the left-hand side of the SR (4) with the small coefficient, proportional to $(m_{1\frac{1}{2}^+} - m_2)\alpha_{21}$. At the same time the contribution from $\frac{1}{2}^+ \to \frac{1}{2}^-$ - transition to the coefficient of T_0 is proportional to $(m_1 + m_2^*)\alpha_{2*1}$, where $\langle B_2^* | H_W^{PC} | B_1 \rangle = \alpha_{2*1}\bar{u}_{2*}\gamma_5 u_1$. Therefore, the SR for T_0 aren't suitable for the calculation of $\langle B_2 | H_W^{PC} | B_1 \rangle$. The structures T_1, T_2, T_3 give three SR which will be designated as I, II, III, respectively. T_1 appears at the bare loop level (fig. 1a). In addition, vacuum expectation value (VEV) of the four-quark operator $\psi\bar{\psi}\psi\bar{\psi}$ gives also large contribution (fig. 3a,b). Relative largeness of the latter is connected with the loss of two small loop factors $(16\pi^2)^{-1}$. It is essential that the graphs of figs. 1a and 3 are IR stable at $Q^2 = 0$. The situation changes for the SR II and III. It is the contribution of operators $\psi\bar{\psi}$ and $\psi\bar{\psi}\psi\bar{\psi}\psi\bar{\psi}$ which is characterized by loss of loop smallness in this case (fig. 4). However, the diagram of fig. 4c essentially includes at $Q^2 = 0$ the long-distance dynamics. Besides, the reliability of factorization hypothesis for the six-quark VEV is not so well established as for the four-quark one. So SR II and III seem to be less confident than I. However, they are consistent with I as we shall show further. Detailed numerical results are given for the SR I.

4.2. Parity violating part of the correlator.

Independent structures are $T_i\gamma_5$ in this case, $i = 0 \div 3$. Define the matrix element of H_W^{PV} between the virtual baryon states as the constant β_{21} of two-particle γ_5-vertex in

Feynman graphs including baryons (fig. 5). Now it is the structures $T_0\gamma_5$ and $T_2\gamma_5$ which are saturated by the transition $\frac{1}{2}^+ \to \frac{1}{2}^+$. Corresponding SR show that β_{21} is equal to zero in SU(3) limit. At small departures from SU(3) symmetry we get among others the terms proportional to $(t_1 - t_2)$. Dependence of these terms upon given by hand relation between t_1 and t_2 prevents from giving an accurate estimate of β_{21} in this case.

5. Sum rules (SR) and fitting procedure

First, consider the matrix elements of I_3 for $\Sigma^+ \to p$ transition. Introduce three invariant functions $k_i(S_1, S_2)$, $i = 1,2,3$:

$$\int \langle 0|T\{\eta_2(y) I_3(0) \bar{\eta}_1(x)\}|0\rangle \exp(iq_2 y - iq_1 x) \cdot d^4x d^4y = \frac{\pi^4}{(2\pi)^{10}}\left[k_1(S_1,S_2)T_1 - k_2(S_1,S_2)T_2 - k_3(S_1,S_2)T_3\right] \quad (12)$$

Then the S-wave contribution of interest is

$$A(\Sigma_0^+) = A(t_1,t_2) \equiv \frac{cs}{64\pi^2 m_\pi^2 f_\pi} \frac{a_3(M)}{\beta_\Sigma \beta_N} t_1 t_2 \exp\left(\frac{m_\Sigma^2}{t_1} + \frac{m_N^2}{t_2}\right) \cdot \begin{cases} \frac{2}{m_\Sigma + m_N} k_1(t_1,t_2) \\ k_2(t_1,t_2) \\ \frac{2}{(m_\Sigma + m_N)^2} k_3(t_1,t_2) \end{cases} \quad (13)$$

Consider the following VEV's:I, $\langle G^2 \rangle$, $\langle \psi\bar{\psi}\psi\bar{\psi} \rangle$, $\langle \psi\bar{\psi}\psi G\bar{\psi} \rangle$, $\langle \psi\bar{\psi} \rangle$, $\langle \psi G\bar{\psi} \rangle$ (we denote $\psi\bar{\psi}\psi\bar{\psi} \equiv \psi_i^a \bar{\psi}_k^b \psi_\ell^c \bar{\psi}_m^d$ etc.). Two last contribute into k_2, k_3 (in sect. 7 operator $\psi G G\bar{\psi}$ is also considered). Third and fourth VEV's are estimated by factorization. Taking into account the anomalous dimensions is made as in ref. [2]; the anomalous dimension of operator averaged by factorization is put to be equal to the sum of the anomalous dimensions of

factors. Calculation of diagrams including emission of soft gluons is performed in the fixed point gauge [4]. The coordinate origin can be chosen either in H_w or, to check the answer, in $\overline{\eta}_1$ or η_2. The result is

$$k_1 = \frac{6}{5}\frac{t_1^2 t_2^2}{t_1+t_2} L^{-4/9} + \frac{1}{6} b \frac{(t_1-t_2)^2}{t_1+t_2} L^{-4/9} +$$
$$+ \frac{16}{3} a^2 L^{+4/9}\left[\frac{t_1^2+t_2^2}{2t_1t_2} + \frac{t_1t_2}{(t_1+t_2)^2}\right] +$$
$$+ \frac{1}{9} a_g a\left[\frac{10}{t_1+t_2} + \frac{t_1^2+t_2^2}{(t_1+t_2)t_1t_2} + \frac{5}{2}\frac{t_1+t_2}{t_1t_2} -\right.$$
$$\left. - \frac{10t_2+13t_1}{t_2^2} - \frac{10t_1+13t_2}{t_1^2} - 5I(Q^2)\right],$$
$$I(Q^2) = \int \frac{dt_3}{t_3} \frac{(t_1+t_2)\exp(-Q^2/t_3)}{(t_1+t_2+t_3)^2} \qquad (14)$$
$$k_2 = \frac{8}{3} a \frac{t_1t_2}{t_1+t_2} + a_g L^{-4/9}\left[\frac{1}{3} - \left(\frac{t_1-t_2}{t_1+t_2}\right)^2\right]$$
$$k_3 = 4a t_1t_2 \frac{t_1^2+t_2^2}{(t_1+t_2)^2} + a_g \cdot 0$$

Here $L = \alpha_s(\mu)/\alpha_s(M) = \ln(M/\Lambda)/\ln(\mu/\Lambda)$, μ is the normalization point of OPE, μ = 0.5 GeV [1], Λ = 0.15 GeV, $a = -(2\pi)^2\langle\bar\psi\psi\rangle = 0.546\ GeV^3$, $a_g = -(2\pi)^2\langle g\bar\psi i\sigma_{\mu\nu}t^n\psi G^n_{\mu\nu}\rangle$, $b = \langle g^2G^2\rangle$ = 0.5 GeV^4, $\sigma_{\mu\nu} = \frac{1}{2}[\gamma_\mu,\gamma_\nu] = \frac{1}{2}(\gamma_\mu\gamma_\nu - \gamma_\nu\gamma_\mu)$

The value $I(Q^2)$ in k_1 diverges logarithmically at $Q^2 \to 0$. On the other hand, it is clear that the Q^2 dependence is stabilized at $Q^2 \sim m_4^2 \sim 1\ GeV^2$ where m_4 is the mass of the lower state in the four-quark channel. Then

$$I(Q^2) = \frac{1}{t_1+t_2} \ln\frac{t_1+t_2}{m_4^2} \qquad (15)$$

with logarithmic accuracy. In another way of estimating we single out the pole contribution of the form $C\cdot(Q^2+m_4^2)^{-1}$ in $I(Q^2)$ and restrict ourself by it at $Q^2 = 0$. To suppress

the contribution of higher states in $I(Q^2)$ we apply the Borel transformation in Q^2. Constant C is estimated at the Borel parameter $t_3 = m_4^2$ and we get at $t_1 = t_2 = 2t$:

$$I(Q^2) \xrightarrow{Q^2\to 0} \frac{t_1+t_2}{(t_1+t_2+t_3)^2}\frac{t_3}{m_4^2}\exp\left(\frac{m_4^2}{t_3}\right) = \qquad (16)$$
$$= \frac{e}{4t}\eta^2,\ \eta = \frac{4t}{4t+m_4^2} = 1 - \frac{m_4^2}{4t} + \ldots \approx 1$$

In both the methods of estimating we obtain the divergent at $Q^2 \to 0$ term being finally reduced to the contribution (of large distances) of order of 10% to the full correction due to $\langle\psi\bar\psi\psi G\bar\psi\rangle$.

As a result, we come to the following SR for $A(\Sigma_o^+)$ at $t_1 = t_2 = 2t = 2M^2$ and for $\hat\beta^2$ [2]:

$$A(\Sigma_o^+) = A(t) \equiv \frac{cs}{16\pi^2 m_\pi^2 f_\pi}\frac{a_3(M)}{\beta_\Sigma\beta_N}\exp\left(\frac{\overline{m^2}}{t}\right)\cdot$$
$$\cdot\frac{2}{m_\Sigma+m_N}\cdot t^2 k_1,\ \overline{m^2} = \frac{1}{2}(m_\Sigma^2+m_N^2),$$
$$k_1 = \frac{24}{5}\left[t^3 + \frac{25}{18}a^2\left(1-\frac{1}{3}\frac{m_o^2}{t}\right)\right], \qquad (17)$$
$$\hat\beta^2\exp\left(-\frac{m^2}{t}\right) = \frac{1}{2}\left[t^3 + \frac{24}{18}a^2\left(1-\frac{1}{4}\frac{m_o^2}{t}\right)\right],$$
$$\langle g(\bar\psi i\sigma_{\mu\nu}t^n G^n_{\mu\nu}\psi)(\bar\psi\psi)\rangle \equiv m_o^2\langle\bar\psi\psi\rangle^2$$

where renormalization group factors are omitted for brevity. Pay attention to the fact that the ratios of the power corrections to the asymptotic term are almost the same for k_1 and for $\hat\beta^2$. Therefore, the dependence of the resulting $A(\Sigma_o^+)$ on the VEV's is comparatively week.

Accounting for the continuum contribution in the triangular version (6a) leads to the following substitution in $t^2k_1(t)$ (17):

$$t^{n+1} \Rightarrow t^{n+1}E_{n+1}\left(\frac{s_o}{t}\right) \equiv \frac{1}{n!}\int_0^{s_o} s^n ds \exp\left(-\frac{s}{t}\right) \qquad (18)$$

Formally the same substitution must be done in $\tilde{\beta}^2$ where now S_0 is the one-dimensional continuum threshold.

We take three values for m_0^2 : 0 , 0.6 and 1 GeV^2. In table 1 the residues $\tilde{\beta}^2$ of baryons are presented, These are calculated utilizing the experimental masses of baryons in the SR presented in Appendix A. We put m_s = 150 MeV, f = -0,2.

Consider the case m_0^2 = 1 GeV^2 which is the worst among studied ones in the sense of the value of power correction. The dependence $A(\Sigma_0^+) = A(t)$ is depicted graphically in fig. 7 at three values of threshold S_0 (in the triangular version of continuum). At S_0 = 2.1 GeV^2 we observe the good fit $A(t) \approx$ const. Estimates show that asymptotic term is almost completely ($\geq$95%) compensated by continuum at this S_0 giving finally 10÷20% of the whole answer. As a result, the term due to $\langle\psi\bar{\psi}\psi\bar{\psi}\rangle$ dominates the answer. It grows with t as t^2. In the SR II or III the term due to $\langle\psi\bar{\psi}\rangle$ is main growing with t as t^3 or t^4 , respectively, and therefore being more strongly suppressed by continuum. As a result, the answer is less sensitive to the value of the following corrections in the SRI, in that we see once more advantage of this SR. The ratio of the correction due to $\langle\psi\bar{\psi}\cdot\psi G\bar{\psi}\rangle$ to the main term isn't larger than 25% at $t \geq$ 1 GeV^2, which satisfies the condition of applicability of OPE in this region [1]. The final answer is

$$A(\Sigma_0^+) = 1.60 \qquad (19)$$

The square version for continuum (6b) at $S_{10} = S_{20}$ leads practically to the same answer

$$A(\Sigma_0^+) = 1.59 \qquad (20)$$

Finally, one can study the dependence $A(\Sigma_0^+) = A(t_1, t_2)$ on two variables t_1 , t_2 . Level lines of this function are depicted in figs. 8a,b for two choices of the continuum thresholds (S_{10} , S_{20}) in square version of continuum. In fig. 8b we have the square of the flat region enhancing as compared to fig. 8a. The result reads

$$A(\Sigma_0^+) = 1.49 \qquad (21)$$

This method is in some sense less reliable than the linear one:

platou exists at $t_i \sim m_i^2 \sim$ 1 GeV^2, not at $t = \frac{t_1}{2} = t_2/2 \sim m^2 \sim$ 1 GeV^2, and the power corrections are more essential here.

Thus, the regio.. of fitting the SR exists and the results obtained by different procedures of fitting differ from each other by no more than 10%

6. Corrections to SU(3) symmetry and to the valence quark model

6.1. Corrections to SU(3) symmetry

In SU(3) limit Σ -waves are given by the expressions analogous to (13) and (14) up to the Klebsh-Gordan coefficients so that

$$-\frac{A(\Sigma^-)}{\sqrt{2}} = A(\Sigma_0^+) = -\sqrt{3}\,A(\Lambda^0) = \frac{\sqrt{3}}{2}A(\Xi^-) \qquad (22)$$

Consider operators m_s, $m_s\psi\bar{\psi}$, $m_s\psi G\bar{\psi}$, $m_s\psi\bar{\psi}\psi\bar{\psi}$ and also take into account the terms proportional to $f = \langle(\bar{s}s - \bar{u}u)\rangle / \langle\bar{u}u\rangle \approx \langle(\bar{s}Gs - \bar{u}Gu)\rangle / \langle\bar{u}Gu\rangle$

In doing so for I_3 piece of Σ -waves we get $-A(\Sigma^-)/\sqrt{2} = -A(\Sigma_0^+)$ as before, but expressions for $k_i(t_1, t_2)$ become different for Ξ , Σ and Λ decays. As a result, three different sets of functions $k_{i\Sigma}$, $k_{i\Lambda}$ and $k_{i\Xi}$ arise:

$$\begin{aligned}
k_{1\Sigma} - k_1 &= m_s\left(-\tfrac{1}{3}at - \tfrac{1}{4}a_g\right) + f\left(\tfrac{2}{3}a^2 + \tfrac{10-e\eta^2}{24}\tfrac{a_g a}{t}\right)\\
k_{2\Sigma} - k_2 &= m_s\left(2t^2 + \tfrac{2+2e\eta}{3}\tfrac{a^2}{t}\right) + f\left(\tfrac{4}{3}at + \tfrac{1}{6}a_g\right)\\
k_{3\Sigma} - k_3 &= m_s\left(12t^3 + \tfrac{40+2e\eta^2}{3}a^2\right) + f\cdot 2at^2\\
k_{1\Lambda} - k_{1\Sigma} &= m_s\left(16at - \tfrac{25}{3}a_g\right) + f\left(\tfrac{16}{3}a^2 - \tfrac{27+e\eta^2}{9}\tfrac{a_g a}{t}\right)\\
k_{2\Lambda} - k_{2\Sigma} &= m_s(-4t^2) + f\left(-\tfrac{8}{3}at - \tfrac{1}{3}a_g\right)\\
k_{3\Lambda} - k_{3\Sigma} &= m_s(-24t^3) + f(-8at^2)\\
k_{1\Xi} - k_{1\Sigma} &= m_s\left(-\tfrac{8}{3}at + \tfrac{7}{2}a_g\right) + f\left(8a^2 - \tfrac{73+e\eta^2}{18}\tfrac{a_g a}{t}\right)\\
k_{2\Xi} - k_{2\Sigma} &= m_s\left(-2t^2 - \tfrac{4}{3}\tfrac{a^2}{t}\right) + f\left(-\tfrac{4}{3}at - \tfrac{1}{6}a_g\right)
\end{aligned} \qquad (23)$$

$$k_{3\Xi} - k_{3\Sigma} = m_s(-12t^3 - 8a^2) + f(-4at^2)$$

Here $t_1 = t_2 = 2t$ and for η see (16). SR II and III are considered in the next section. Results of fitting the SR I with the triangular version of continuum are presented in table II for $f = -0.2$, $m_s = 150$ MeV and three values of m_0^2: 0, 0.6 and 1 GeV^2. Given are also the results of calculations in the MIT bag model [14, 15] and in the harmonic oscillator model [16]. Of the values of m_0^2 used the value 0.6 GeV^2 is in the best agreement with the nucleon SR [2]. We see that our results for this m_0^2 are in the best agreement with the latest calculations [16].

As for the full S-waves in the soft pion limit the "penguin" must also be accounted for. We use the experimental fit (11) for that. I_3 and "penguin" S-wave pieces are presented in table 3. Adding them leads to the large as compared to experiment amplitudes A. However, the correction due to the non-zero pion momentum can be essential. Namely, the important role of the pole contribution from the SU(6) multiplet $(\underline{70}, 1^-)$ was revealed in ref. [17]. Since the estimate of ref. [17] is valid within factor of 2, accounting for it has an illustrative character. We give in table 3 the values differing by 20% from those used in [17] to show the principial possibility to fit to the experimental S-waves.

In table 4 presented are P-waves in the ground-state pole approximation. The formulas for this approximation are given in Appendix B. I_3 and "penguin" pieces of commutator term in S-waves are those used in table 3 and are considered separately*. For axialvector coupling we use the measured [19] parameters $d = 0.823$, $f = 0.428$. Table 4 is in accordance with the MIT bag estimates [21] giving essential values for the contribution of the next resonances into $B(\Sigma_0^+)$ and $B(\Sigma_+^+)$ (in case Σ_+^+ it reaches 40% of the whole amplitude B).

*) Stress the following. If the "penguin" piece of S-wave is interpreted as separable contribution of $O_{5,6}$ with H_w normalized in low-energy point then the corresponding pole contribution into P-waves turns out to be just the analogous separable contribution of $O_{5,6}$ into P-waves.

6.2. Matrix elements of I_6.

According to the Pati-Woo theorem [11] matrix elements of I_6 between the one-baryon states vanish due to antisymmetry of the baryon wave function in colour indices in the valence quark model. However, the process of contraction of colour indices is changed in the diagrams like those of fig. 6 with the soft gluon emission, so I_6 begins to contribute. General diagrammatic analysis leads to the following parameterization of I_6 piece in S-waves:

$$\frac{1}{2\sqrt{2}}\delta A(\Sigma_+^+) = \frac{1}{\sqrt{2}}\delta A(\Sigma_-^-) = \delta A(\Sigma_0^+) = \frac{1}{\sqrt{3}}\delta A(\Lambda_-^0) =$$
$$= -\sqrt{\frac{2}{3}}\delta A(\Lambda_0^0) = -\frac{\varepsilon}{4}, \quad \delta A(\Xi_-^-) = \delta A(\Xi_0^0) = 0 \qquad (24)$$

This result is valid for the specific choice of baryon currents (sect. 3). This analysis shows also that ε emerges only if condensates of one (and only one) of the quark fields q_1, q_2 (see fig. 1a) and of one of q_3, q_4 are taken into account $\langle\psi\bar\psi\psi G\bar\psi\rangle$ is the lower dimensional ($d = 8$) VEV contributing to ε. Next VEV's cannot be utilized for calculation of ε since their OPE coefficients are IR divergent in the power manner. The result of calculation of ε due to $\langle\psi\bar\psi\psi G\bar\psi\rangle$ reads as

$$\varepsilon = \frac{cs}{16\pi^2 m_\pi^2 f_\pi}\frac{1}{\tilde\beta_1\tilde\beta_2}a_6(M)\exp\left(\frac{\overline{m^2}}{t}\right)t^2 k_1 \qquad (25)$$
$$k_1 = -\frac{a_g a}{t}\left(2 - \frac{e}{3}\eta^2\right)$$

To estimate ε introduce the continuum threshold s_0. At $t \gg s_0$

$$\varepsilon = -\frac{cs}{16\pi^2 m_\pi^2 f_\pi}\frac{1}{\tilde\beta_1\tilde\beta_2}a_g a\, a_6(\sqrt{s_0})f(t) \qquad (26)$$
$$f(t) = t\,E_1(s_0/t)\exp(\overline{m^2}/t)$$

Choose the equalities $f'(t) = 0$, $f''(t) = 0$ as the conditions of maximal constancy of $f(t)$. We get $t = \infty$, $s_0 = 2\overline{m^2}$.

Note that $S_0 \sim 2$ GeV^2 obtained is quite reasonable, and at $t = \infty$ the higher power corrections vanish. Finally $f(t) = 2\overline{m^2}$. Taking $\overline{m^2} = m_N^2$, $\tilde{\beta}_1 = \tilde{\beta}_2 = \tilde{\beta}_N$ we arrive at

$$\varepsilon \simeq -0.2 m_0^2 / 1\,\text{GeV}^2 \qquad (27)$$

The calculated correction due to I_6 develops itself at experiment as the $\Delta T = 3/2$ pole P-wave amplitudes. The latter are given in table 5. The contribution of separable diagrams into $\Delta T = 3/2$ P-wave amplitudes [9] is also given in table 5. It is seen that taking into account the pole contribution in addition to the separable one improves the agreement with experiment.

7. Consistency of the sum rules (SR)

As we have seen, there are another contributions into S-waves besides that calculated in this paper. So, the question of reliability of calculations is rather important.

Here we consider SR II and III corresponding to the chiral-noninvariant structures T_2, T_3 in the correlator. Consistency of these with SR I is shown. In particular, the duality estimate is obtained from SRI and II. It has the universal form and is compatible with the calculations made. The results of fitting these SR turn out to be also consistent. Finally, correction due to the VEV $\langle \psi G G \bar{\psi} \rangle$ is calculated in two variants of estimating this VEV: 1) in the instanton approximation and 2) by factorization. It's taking into account turns out to change the answer slightly.

7.1. Duality estimate

Consider the limit $t_1, t_2 \to \infty$ in the three-point SR and $t \to \infty$ in $\tilde{\beta}^2(t)$. In this limit the (nonnegative) power of M^2 transmutes to the same power of the continuum threshold S_0. Confine ourself to the main term in both the SR. To cancel the dependence upon S_0 in the final answer the powers of M^2 must be the same in both the SR. There are two possibilities satisfying this condition: the SR I or II can be

taking in the numerator of expression for S-wave, then the SR for $\tilde{\beta}^2$ contributed by the VEV $\langle \psi\bar{\psi} \rangle$ or I, respectively, must be taking in the denominator. It is important, that the power of M^2 in the main term in the SR I is equal to 2 (see sect. 5). Thus, we have in SU(3)-limit:

$$A(\Sigma_0^+) = \frac{cs}{64\pi^2 m_\pi^2 f_\pi} a_3(M) \exp\left(m^2 \frac{t_1+t_2}{t_1 t_2}\right) \cdot \qquad (28)$$

$$\cdot \begin{cases} \frac{1}{m\tilde{\beta}^2} t_1 t_2 k_1 \\ \frac{1}{\tilde{\beta}^2} t_1 t_2 k_2 \end{cases}$$

where

$$t_1 t_2 k_1 = \frac{8}{3} a^2 L^{4/9} \left[t_1^2 + t_2^2 + 2 \left(\frac{t_1 t_2}{t_1+t_2} \right)^2 \right]$$

$$m\tilde{\beta}^2 \exp(-m^2/t) = a t^2 \qquad (29)$$

$$t_1 t_2 k_2 = \frac{8}{3} a \frac{t_1^2 t_2^2}{t_1+t_2}$$

$$\tilde{\beta}^2 \exp(-m^2/t) = \frac{1}{2} t^3 L^{-4/9}$$

Introduce the duality interval S_0 in each of the baryon channels. Then, tending $t_1, t_2, t \to \infty$ in (28), (29) we find

$$A(\Sigma_0^+) = \frac{1}{3} cs \frac{f_\pi}{(m_u+m_d)_\mu} \qquad (30)$$

the result, identical for I and II SR. Here we have used the result of PCAC $\langle \bar{\psi}\psi \rangle = -\frac{1}{2} m_\pi^2 f_\pi^2 (m_u+m_d)^{-1}$ [7], μ is the normalization point of OPE. Note that $(m_u+m_d)_\mu \cdot a_3(\mu)$ is renorminvariant. Estimate is given for $cs = 0.215$, $f_\pi = 133$ MeV, $(m_u+m_d)_{0.5\,\text{GeV}} = 11$ MeV, $\Lambda = 0.15$ GeV, $a_3(80\ \text{GeV}) = 1$.

Notice that universality of the estimate (30) for the SR I and II is the consequence of the factorization of four-quark VEV $\langle \psi\bar{\psi}\psi\bar{\psi} \rangle$ entering k_1.

7.2. Fitting procedure

As was mentioned in sect. 4, the contribution of six-quark

VEV (fig. 4b,c) contains no small loop factors, at the same time it's OPE coefficients are strongly IR unstable. True, the graph of fig. 4b can be estimated perturbatively, giving for the sum of it with the main term due to :

$$k_2 = \frac{8}{3} a t \left(1 + \frac{1}{3} a^2 t^{-3}\right) \qquad (31)$$

in the framework of the factorization of six-quark VEV. The correction obtained to the main term is of order of 10÷20% and one can expect that the full correction due to $\langle \psi\bar\psi\psi\bar\psi\psi\bar\psi\rangle$ is of the same order of magnitude. The accuracy of consistency with the SR I must be the same.

We take $k_{2\Sigma}$ from (14), (23) and write out also the SR for $\tilde\beta_\Sigma^2$, $\tilde\beta_N^2$ [2]:

$$A(\Sigma_o^+) = \frac{cs}{16\pi^2 m_\pi^2 f_\pi} \frac{a_s(M)}{\tilde\beta_\Sigma \tilde\beta_N} \exp\left(\frac{\overline{m^2}}{t}\right) t^2 k_2$$

$$k_2 = \frac{8}{3} a t \left(1 + \frac{1}{2} f + \frac{3}{4} \frac{m_s}{a} t + 0.9 \frac{m_s a}{t^2}\right) + \frac{a_g}{3} \qquad (32)$$

$$m_N \tilde\beta_N^2 \exp(-m_N^2/t) = a t^2$$

$$m_\Sigma \tilde\beta_\Sigma^2 \exp(-m_\Sigma^2/t) = a t^2 \left(1 + f + \frac{m_s}{a} t + \frac{4}{3} \frac{m_s a}{t^2}\right)$$

We put a_g/a = 1 GeV^2. To eliminate the dependence of final answer upon the scale of $\langle\bar\psi\psi\rangle$ and of other chiral-noninvariant VEV's we have expressed both k_2 and $\tilde\beta^2$ in (32) through these VEV's. The fact is that the structures of different chirality in two-point correlator give rise to somewhat different $\tilde\beta^2$. Namely, we have $\tilde\beta^2$ = 0.97 from (32) which is 25% smaller than the value 1.26 given by the SR with asymptotic loop (table 1). If this difference is due to the inaccuracy in the determination of the scale of VEV's, it turns out to be unessential in our approach. Note also some stability of the result with respect to the choice of SU(3) -- violation parameters f, m_s, which is seen from the following formal anzats:

$$\sqrt{m_\Sigma m_N} \exp(-\overline{m^2}/t) \tilde\beta_\Sigma \tilde\beta_N = a t^2 \left(1 + \frac{1}{2} f + \frac{1}{2} \frac{m_s}{a} t + \frac{2}{3} \frac{m_s a^2}{t^2}\right) \qquad (33)$$

which should be compared with k_2 from (32). For f= -0.2. m_s = 150 MeV, we find:

$$A(\Sigma_o^+) = 1.48 \qquad (34)$$

This value should be compared with $A(\Sigma_o^+) = 1.44 \div 1.77$ from table 2 at $m_o^2 = 1 \div 0.6$ GeV^2.

The SR III are the least reliable ones due to the high power of t being equal to 4 in the main term in these SR. As a result, the main term is strongly compensated by continuum and the answer is sensitive to the values of subsequent corrections, of which the nearest one due to $\langle\bar\psi G\psi\rangle$ vanishes. Therefore, for example, accounting for the $SU(3)$ -violating VEV's changes the answer for A (Σ_o^+) from 0.4 to 1.1, i.e. more than 2.5 times. Here we can state only an order-of-magnitude consistency of the SR.

7.3 Correction due to $\langle\psi GG\bar\psi\rangle$

There are several VEV's os zero colour and Lorentz spin differing by the method of contraction of indices in $\langle \psi_i^a G_{\mu\nu}^m G_{\lambda\rho}^n \bar\psi_k^b\rangle$. To calculate their contribution into correlator in the instanton approximation we expand the correlator in the instanton field up to the power term determined by the VEV's $\langle m_q \psi\bar\psi\psi\bar\psi\rangle$, $\langle \nabla_\mu \psi\bar\psi\psi\bar\psi\rangle$ and $\langle\psi GG\bar\psi\rangle$. Then we find and subtract from this term its part caused by $\langle m_q \psi\bar\psi\psi\bar\psi\rangle$ and $\langle \nabla_\mu \psi\bar\psi\psi\bar\psi\rangle$.

At the first step we use expansion in the quark mass m_q of the quark propagator in the instanton field [12]. We get the diagrams like those of fig. 9, where P_o is the zero fermionic mode [12]. Calculations give

$$m\tilde\beta^2 \exp\left(-\frac{m^2}{M^2}\right) = (2\pi)^2 M^4 \int dn(\rho) \frac{2}{m_q} I\left(\frac{2}{\rho M}\right)$$

$$I(x) = \left[1 + 0\cdot x^2 - \frac{1}{5} x^4\right] + \frac{2}{5} x^4 = \qquad (35)$$

$$= 1 + 0\cdot x^2 + 0.20 x^4$$

$$k_2 = \frac{8}{3} (2\pi)^2 M^2 \int dn(\rho) \frac{2}{m_q} J\left(\frac{2}{\rho M}\right),$$

$$J(x) = \left[1 + \frac{1}{8} x^2 - \frac{10 + 3e\eta}{80} x^4\right] + \frac{3}{8} x^4 \approx$$

$$\approx 1 + 0.125 x^2 + 0.15 x^4$$

For η see (16). Here the terms in square brackets in

I, J , correspond to the diagrams with one P_o (fig. 9a,b) while the last terms are due to those with two P_o plus quark mass insertion (fig. 9c,d). These last terms correspond exactly to $\langle m_q \psi\bar\psi\psi\bar\psi\rangle$ piece and must be subtracted at the second stage.

As for the $\langle \nabla_\mu \psi\bar\psi\psi\bar\psi\rangle$ piece, these VEV's are reduced by equations of motion to $\langle m_q \psi\bar\psi\psi\bar\psi\rangle$ and some minimal set of VEV's including derivatives. The latter are chosen as $\langle(\bar\psi \overleftrightarrow{\nabla}_\mu \Gamma_A \psi)(\bar\psi\Gamma_B\psi)\rangle$ and $\langle(\bar\psi \overleftrightarrow{\nabla}^n_\mu \Gamma_A\psi)(\bar\psi\Gamma_B t^n\psi)\rangle$ where Γ_A , Γ_B are bispinor Fierz matrices, A,B = 1÷16, $2t^n$ are the Gell-Mann matrices in colour space, $\overleftrightarrow{\nabla}_\mu \equiv \overrightarrow{\nabla}_\mu - \overleftarrow{\nabla}_\mu$, $\overleftrightarrow{\nabla}^n_\mu \equiv t^n\overrightarrow{\nabla}_\mu - \overleftarrow{\nabla}_\mu t^n$ and indices A,B,μ are contracted in all possible ways to give zero Lorentz spin. Saturating these VEV's by instanton one arrives at

$$\langle(\nabla_\mu u)^a_i \bar u^b_k d^c_\ell \bar d^d_m\rangle = -i\,\frac{\langle m(\bar uu)(\bar dd)\rangle}{64\cdot 9}\cdot$$
$$\cdot(\delta^{ab}\delta^{cd}+\tfrac{3}{8}t^{nab}t^{ncd})\cdot(\gamma_{\mu ik}\delta_{\ell m}+\gamma_{\mu 5ik}\gamma_{5\ell m} \tag{36}$$
$$-\gamma_{5ik}\gamma_{\mu 5\ell m}-\tfrac{1}{3}\sigma_{\rho\mu 5ik}\gamma_{\rho 5\ell m}),\ \gamma_\mu\equiv\gamma_\mu\gamma_5,\ \sigma_{\rho\mu 5}\equiv$$
$$\equiv\sigma_{\rho\mu}\gamma_5$$

which allows one to find the $\langle \nabla_\mu \psi\bar\psi\psi\bar\psi\rangle$ piece in I, J:

$$I_{\langle\nabla\psi^4\rangle} = -\frac{1}{20}x^4$$
$$J_{\langle\nabla\psi^4\rangle} = -3\,\frac{3\varepsilon\eta-1}{160}x^4 \tag{37}$$

Subtracting (37) from the bracketed terms in I,J (35), we get the correction due to $\langle\psi GG\bar\psi\rangle$ in the single instanton approximation:

$$\tilde\beta^2 \sim I = 1+0\cdot x^2 - 0.15\,x^4$$
$$k_2 \sim J = 1+0.125x^2-0.10\,x^4 \tag{38}$$

Typical ρ is $(600\ \text{MeV})^{-1}$ [13]. The corrections obtained are identical in $\tilde\beta^2$ and k_2 up to a factor of 1.5, so $A(\Sigma^+_o)$ remains unchanged within 5%. Note that the correspondence between the corrections in $\tilde\beta^2$ and k_2 keeps at each step of our calculation.

Estimate of the $\langle\psi GG\bar\psi\rangle$ correction within factorization hypothesis is achieved by treatment of the graphs of fig. 10a,b. The two-point correlator was considered in [2]. The result has the form

$$I = 1+0\cdot\frac{a_q}{aM^2}-\frac{1}{18}\frac{b}{M^4}$$
$$J = 1+\frac{1}{8}\frac{a_q}{aM^2}+\left(-\frac{1}{8}+\frac{e\eta}{36}\right)\frac{b}{M^4}\approx \tag{39}$$
$$\approx 1+\frac{1}{8}\frac{a_q}{aM^2}-\frac{1}{20}\frac{b}{M^4}$$

Again, accounting for this correction leaves the answer practically unchanged.

8. Conclusion

We have considered quite definite pieace of S -wave amplitudes in the framework of QCD SR. With the values obtained, we have also calculated the pole contribution into $\Delta T = 1/2$ and $\Delta T = 3/2$ P -wave amplitudes. It turns out that some phenomenological or model-inspired accounting for other pieces of amplitudes considered can, in principle, give reasonable agreement with experiment. In calculations performed, the complex VEV's $\langle\psi\bar\psi\psi\bar\psi\rangle$ and $\langle\psi\bar\psi\psi G\bar\psi\rangle$ play definite role. These VEV's are estimated using the factorization hypothesis.

We have shown that the results for the S -wave amplitudes given by QCD SR are quite unambiguous (within 10-15%). In particular, we have checked consistency of the SR and stability of the results with respect to the choice of fitting procedure.

We have studied in detail power corrections in the region $d \le 8$ where OPE is applicable. We have shown that considered VEV's change the numerator (three-point SR) and the denominator (two-point SR) in analogous way, so that the answer weakly depends upon these VEV's, at least, in qualitative aspect. One can say in this sense that S -wave piece calculated is low sensitive to the properties of QCD vacuum. Using QCD SR for analysis of the "penguin" mechanism where the long-distance physics is essential can be the next step.

In conclusion, the author is indebted to V.L. Chernyak, I.B. Khriplovich, O.V. Zhirov, A.R. Zhitnitsky and I.R. Zhitnitsky for numerous helpful discussions and especially to A.I. Vainshtein for the detailed analysis of the work.

Appendix A

SR for baryon residues into currents used have the form:

$$2\tilde{\beta}_N^2 \exp(-m_N^2/t) = t^3 E_3 L^{-4/9} + \frac{1}{4} b t E_1 L^{-4/9} + \frac{4}{3} a^2 (L^{4/9} - m_0^2/4t) \quad (1A)$$

$$2\tilde{\beta}_\Sigma^2 \exp(-m_\Sigma^2/t) = f(t) - 2m_s a t E_1 L^{-4/9} \quad (2A)$$

$$2\tilde{\beta}_\Lambda^2 \exp(-m_\Lambda^2/t) = f(t) + 2m_s a \left(\frac{1}{3} - f\right) t E_1 L^{-4/9} + \frac{16}{9} a^2 L^{4/9} f \quad (3A)$$

$$2\tilde{\beta}_\Xi^2 \exp(-m_\Xi^2/t) = f(t) + \frac{4}{3} a^2 (2f + f^2) L^{4/9} \quad (4A)$$

These were obtained, with exception of (3A), in ref. [2].

Appendix B

P-waves in the ground-state pole approximation have the form according to ref. [20]

$$B(\Sigma_+^+) = -\frac{m_\Sigma + m_N}{m_\Sigma - m_N} \sqrt{2} \left[(d+f) A(\Sigma_0^+) + \frac{f}{\sqrt{2}} A(\Sigma_-^-) + \frac{\varkappa}{\sqrt{3}} d A(\Lambda_-^0) \right] \quad (1B)$$

$$B(\Sigma_0^+) = \frac{m_\Sigma + m_N}{m_\Sigma - m_N} (f-d) A(\Sigma_0^+) \quad (2B)$$

$$B(\Sigma_-^-) = \frac{m_\Sigma + m_N}{m_\Sigma - m_N} \left[f A(\Sigma_-^-) - \sqrt{\frac{2}{3}} \cdot \varkappa d A(\Lambda_-^0) \right] \quad (3B)$$

$$B(\Lambda_-^0) = \frac{m_\Lambda + m_N}{m_\Sigma - m_N} \left[\varkappa (d+f) A(\Lambda_-^0) + \frac{2d}{\sqrt{3}} A(\Sigma_0^+) \right] \quad (4B)$$

$$B(\Lambda_0^0) = \frac{m_\Lambda + m_N}{m_\Sigma - m_N} \left[-\frac{\varkappa}{\sqrt{2}} (d+f) A(\Lambda_-^0) + \frac{d}{\sqrt{3}} A(\Sigma_-^-) \right] \quad (5B)$$

$$\varkappa = \frac{m_\Sigma - m_N}{m_\Lambda - m_N}$$

$$B(\Xi_-^-) = -B(\Xi_0^0)\sqrt{2} = \frac{m_\Xi + m_\Lambda}{m_\Xi - m_\Lambda} A(\Xi_-^-) \cdot \begin{cases} (f-d) & (6B) \\ (f - d/3) & (7B) \end{cases}$$

The difference between (6B) and (7B) accounting for $I_{3,6}$ and "penguin" respectively is connected with that the Σ^--pole contributes in (7B), not in (6B).

References

1 M.A. Shifman, A.L. Vainshtein and V.L. Zakharov, Nucl. physics, B 147 (1979) 385, 448.

2 B.L. Ioffe, Nucl. Phys. B 188 (1981) 317; (E) B 191(1981) 591;
V.M. Belyaev and B.L. Ioffe, preprint ITEP-59 (1982); ZhETF 83 (1982) 876;
V.M. Belyaev and B.L. Ioffe, preprint ITEP-132 (1982); ZhETF 84 (1983) 1236.

3 Chung et al., Nucl. Phys. B 197 (1981) 55.

4 B.L. Ioffe and A.V. Smilga, Phys.Lett. 114B (1982) 353;
V.A. Nesterenko and A.V. Radyushkin, Phys.Lett. 115B (1982) 410;
V.L. Eletsky, B.L. Ioffe and Ya.I. Kogan, Phys. Lett. 122 B (1983) 423.

5 B.L. Ioffe and A.V. Smilga, ZhETF Pisma 37 (1983) 250;
B.L. Ioffe and A.V. Smilga, preprint ITEP-60 (1983);
B.L. Ioffe and A.V. Smilga, preprint ITEP-97 (1983).

6 V.M. Belyaev and Ya.I. Kogan, preprint ITEP-73 (1983); ZhETF Pisma 37 (1983) 611;
V.M. Belyaev and Ya.I. Kogan, preprint ITEP-135 (1983).

7 S. Glashow and S. Weinberg, Phys.Rev. Lett. 20 (1968)224.

8 M.K. Gaillard and B.W. Lee, Phys.Rev. Lett. 33 (1974)108;
G. Altarelli and L. Maiani, Phys. Lett. 52B (1979) 351.

9 A.I. Vainshtein, V.I. Zakharov and M.A. Shifman, ZhETF 72 (1977) 1275.

10 L.B. Okun, Leptons and quarks, (Nauka, Moscow, 1981).

11 J. Pati and C. Woo, Phys. Rev. D3 (1971) 2920.

12 L.S. Brown, R.D. Carlitz, D.B. Creamer and C. Lee, Phys. Lett. 71B (1977) 103;
Phys. Rev. D17 (1978) 1583.

13 E.V. Shuryak, Nucl. Phys. B 203 (1982) 93.

14 H. Galic, D. Tadic and J. Trampetic, Nucl. Phys. B 158 (1979) 306.

15 J.E. Donoghue, E. Golowich, B.R. Holstein and W.A. Ponce, Phys. Rev. D 23 (1981) 1213.
16 S. Avinash, M. Gupta and M.P. Khanna, Phys. Rev. D 29 (1984) 159.
17 A. Le Yaouanc, O. Pene, J.C. Raynal, L. Oliver, Nucl. Phys. B 149 (1979) 321.
18 Particle Data Group, Phys. Lett. 111B (1982).
19 M. Roos, Phys. Lett. 36 B (1971) 130.
20 J. Finjord and M.K.Gaillard, Phys. Rev. D22 (1980) 778.
21 M. Milosevic, D. Tadic and J. Trampetic, Nucl. Phys. B 207 (1982) 461.

Figure captions

Fig. 1. Two types of diagrams appearing in general analysis of the correlator: solid lines denote quarks, dashed lines denote gluons.

Fig. 2. Diagram corresponding to the separable contribution of $O_{5,6}$.

Fig. 3. Diagram proportional to the contribution $\langle\psi\bar{\psi}\psi\bar{\psi}\rangle$ to the correlator.

Fig. 4. Diagrams proportional to the contributions $\langle\psi\bar{\psi}\rangle$ and $\langle\psi\bar{\psi}\psi\bar{\psi}\psi\bar{\psi}\rangle$ to the correlator.

Fig. 5. Two-baryon γ_5 -vertex.

Fig. 6. Diagram proportional to the contribution $\langle\psi\bar{\psi}\psi G\bar{\psi}\rangle$ to the correlator.

Fig. 7. Function $A(\Sigma_0^+) = A(t)$ at three values of the continuum threshold s_0 .

Fig. 8. Function $A(\Sigma_0^+) = A(t_1,t_2)$ at two values of the pair of the continuum thresholds (s_{10} , s_{20}).

Fig. 9. Diagrams corresponding to two- and three-point correlators in the instanton field.

Fig. 10. Diagrams proportional to the contribution $\langle\psi GG\bar{\psi}\rangle$ to the two- and three-point correlators.

Table captions

Table 1. Baryon residues into currents used.

Table 2. S -waves in the soft-pion approximation and without accounting for the "penguin" contribution.

Table 3. Full S -waves.

Table 4. P -waves in the ground-state pole approximation.

Table 5. Deviations from $\Delta T = 1/2$ rule for P -waves.

Table 1.

m_0^2, GeV^2	$\tilde{\beta}^2$, GeV^6			
	Ξ	Σ	Λ	N
0	2.45	1.80	1.60	1.10
0.6	2.36	1.72	1.45	1.01
1	2.32	1.64	1.40	0.97

Table 2.

Mode	Amplitude A					
	QCD, m_0^2/1GeV^2=			Quark models		
	0	0.6	1	[16]	[15]	[14]
Σ_0^+	2.14	1.77	1.44	1.81	1.27	1.52
$-\Lambda_-^0$	1.05	0.80	0.58	0.99	0.71	0.88
Ξ_-^-	2.64	2.33	2.09	2.06	1.46	1.75

Table 3.

Mode	Amplitude A				
	Commutator		$(\overline{70}, 1^-)$	Full	Experi-
	I_3	penguin	[17]	S-wave	ment [18]
Σ_0^+	1.8	0.9	-1.3	1.4	1.48±0.05
$-\Lambda_-^0$	0.8	1.1	-0.5	1.4	1.48±0.01
Ξ_-^-	2.3	1.3	-1.2	2.4	2.04±0.01

Table 4.

Mode	Amplitude B			
	I_3	penguin	Full P-wave	Experi- ment [18]
Σ_+^+	-11.0	0	-11.0	-19.07±0.07
Σ_0^+	-6.0	-3.1	-9.1	-12.04±0.58
Σ_-^-	-2.6	+4.3	+1.7	+0.65±0.07
Λ_-^0	+2.0	-9.1	-7.1	-9.38±0.24
Ξ_-^-	-10.7	+2.5	-8.2	-7.49±0.28

Table 5.

Mode	Amplitude B			
	Pole	Separable [9]	Full P-wave	Experiment [18]
$\Lambda_-^0 + \Lambda_0^0\sqrt{2}$	0.44	-0.95	-0.51	0.03±1.03
$\Xi_-^- + \Xi_0^0\sqrt{2}$	0	0.23	0.23	0.39±0.75
$\Sigma_-^- + \Sigma_0^+\sqrt{2}$ - $-\Sigma_+^+$	0.58	0.49	1.07	2.76±0.96

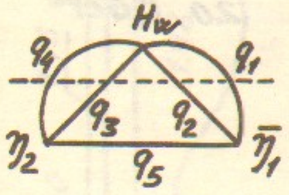

(a)

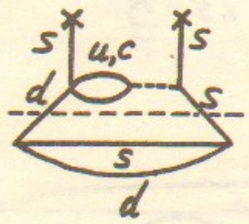

(b)

Fig. 1

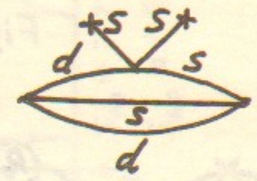

Fig. 2

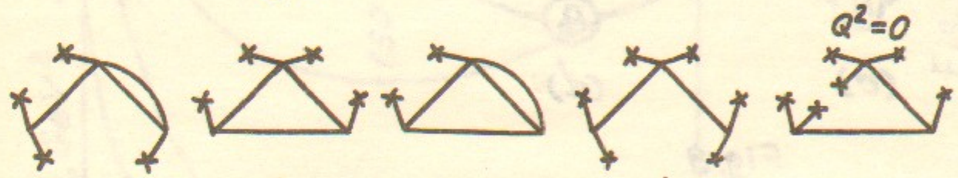

(a) (b) (a) (b) (c)

Fig. 3

Fig. 4

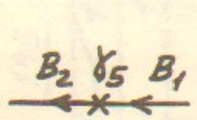

Fig. 5

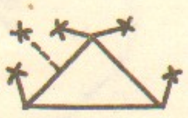

Fig. 6

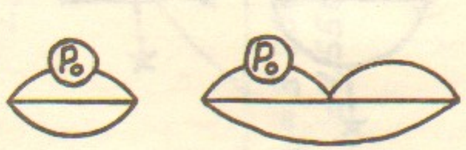

(a) (b)

Fig. 9

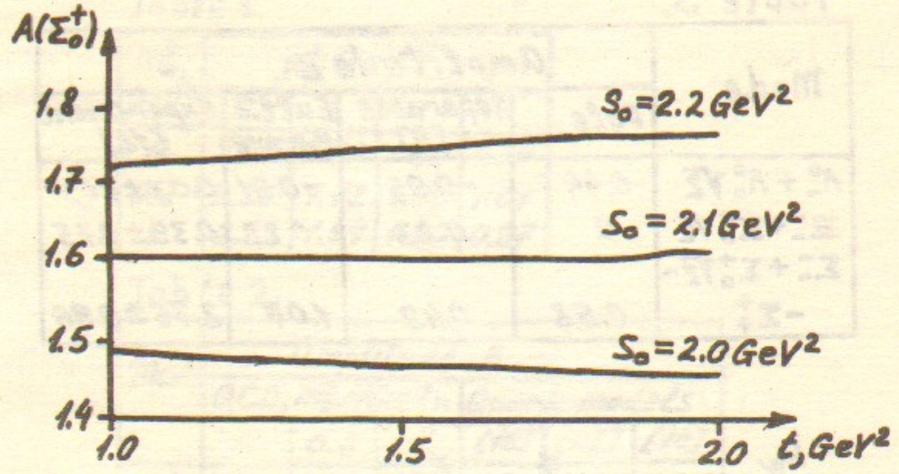

Fig.7

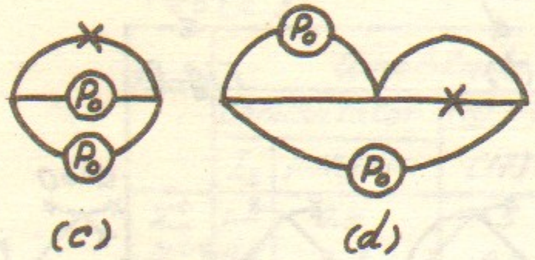

Fig. 9

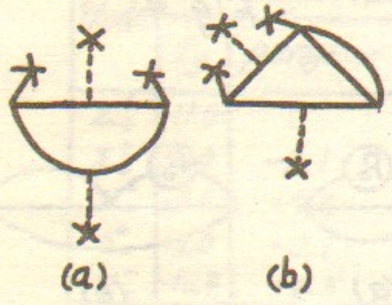

Fig. 10

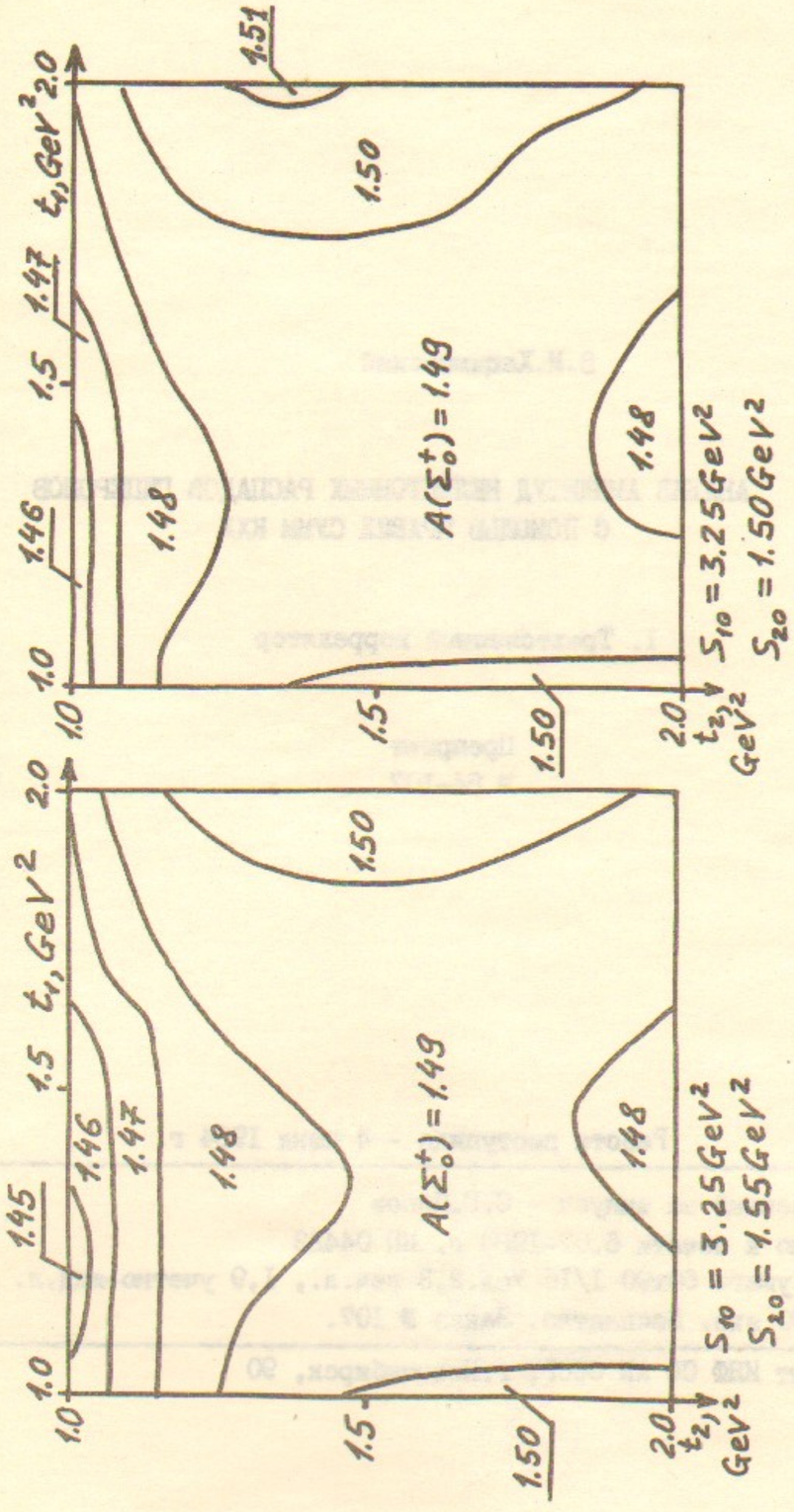

Fig. 8

В.М.Хацимовский

АНАЛИЗ АМПЛИТУД НЕЛЕПТОННЫХ РАСПАДОВ ГИПЕРОНОВ С ПОМОЩЬЮ ПРАВИЛ СУММ КХД

I. Трехточечный коррелятор

Препринт
№ 84-I07

Работа поступила - 4 июня I984 г.

Ответственный за выпуск - С.Г.Попов
Подписано к печати 6.07-I984 г. МН 04423
Формат бумаги 60x90 I/I6 Усл.2,3 печ.л., I,9 учетно-изд.л.
Тираж 290 экз. Бесплатно. Заказ № I07.

Ротапринт ИЯФ СО АН СССР, г.Новосибирск, 90